12th ANKARA INTERNATIONAL AEROSPACE CONFERENCE **AIAC-2023-061**
13-15 September 2023 - Online, Ankara, TURKEY

DESIGN IMPROVEMENT OF THE DISPOSABLE NOZZLE HOLDER USING TOPOLOGY OPTIMIZATION

Halil İbrahim KOÇLUK[1]
Roketsan Missiles Inc.
Ankara, Turkey

Erdem ACAR[2]
TOBB University of Economics and Technology
Ankara, Turkey

ABSTRACT

In this study, it is aimed to improve the design of the nozzle holder parts used in Two-stage nozzle engine systems by using topology optimization. The holding parts designed for the separable nozzle must first keep the engine internal pressure up to a certain level. Then the holders for the second phase are separated from the system by the special screw and the engine switches to the second phase. In this study, for an efficient design, the mass and dimensions of the holders are determined through topology optimization. The obtained mass-improved part will be subjected to the strength test in the hydrostatic test setup, and the topology optimization data will be validated.

INTRODUCTION

Two-stage rockets use a launch engine with two separate combustion chambers to reach the speed of sound. After the launch phase, the internal accelerator accelerates the rocket up to a certain speed. After this stage, the second phase is started. Because the operating pressure of the launch engine's fuel is higher, the system requires a smaller diameter nozzle throat in launch mode, while in second mode this diameter needs to be enlarged. For this reason, the nozzle throat diameter should be changed during the transition from the ejection stage to the cruising stage. The nozzle must be discarded for this transition [WEBSTER, F., 1978]. In this project, the holding parts designed for the disposable nozzle must first hold the pressure up to a certain level. Then, the holders for the second phase are separated from the system with the screws that explode. In this study, for an efficient design, the mass and dimensions of the holders are determined through topology optimization.

Two-stage engines generally consist of an air intake, a combustion chamber and a nozzle. In order for Two-stage engines to work, either the platform must be brought to the speed of sound with the help of another flying platform or it must be increased to sound speed levels by means of the engine. In order for the engine to reach the desired thrust during the first launch, a smaller diameter nozzle is used. In the second phase, the nozzle diameter is enlarged [Fry, R.S., 2004; Aminjan, K.K, 2022]. The aim of this study is to bring the nozzle holder parts to the optimum dimensions and mass through topology optimization to ensure the change in nozzle

[1] Design Engineer, Email: ibrahim.kocluk@roketsan.com.tr
[2] Prof., Department of Mechanical Engineering, Email: acar@etu.edu.tr

diameter, and to validate the analysis by conducting tests. Figure 1 shows a sectional view of the design in which the disposable nozzle assembly is fixed with the holder and clamp parts.

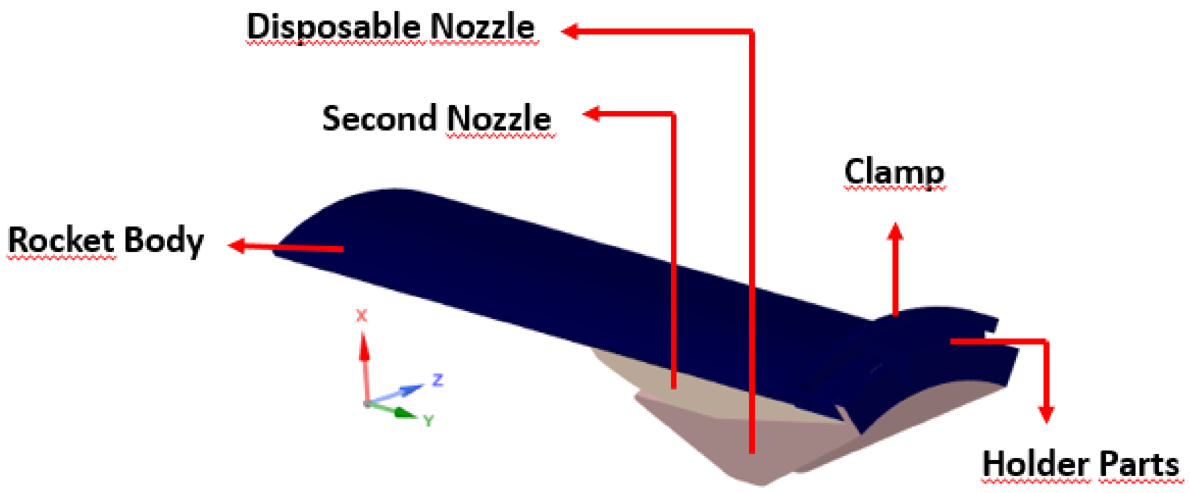

Figure 1. Sectional view of the model

METHOD

Workbench Structural Analysis

The best way to see if the load-bearing parts maintain their structural integrity before production is to analyze the modeled parts. In this study, first of all, the desired holding parts are modeled using the CATIA software. The conceptual design model is analyzed using the ANSYS finite element analysis (FEA) software and it is evaluated whether the part is suitable for strength or improvements are required. After obtaining the final design that maintains its strength at the desired pressure level, topology optimization will be applied as in Ref. [Jiang, T., & Chirehdast, M.,1996; Rozvany, G. I., 2008]. In topology optimization, the minimum weight will be sought and a constraint will be used on the safety factor. The final model obtained will be tested by creating appropriate test conditions, and the suitability of the results obtained in the analysis and the test results will be evaluated.

The slice image of the FEA model is given in Figure 2 To shorten the analysis time and increase the accuracy of the results obtained by using more mesh, 1/6 slices are taken from the model. Firstly, a simplification was made from model 1 to model 2 in Figure 2 to improve the analysis in terms of time. Then, model number 2 was changed to model number 3 in order to get better results by increasing the mesh number and to save time by simplifying the geometry.

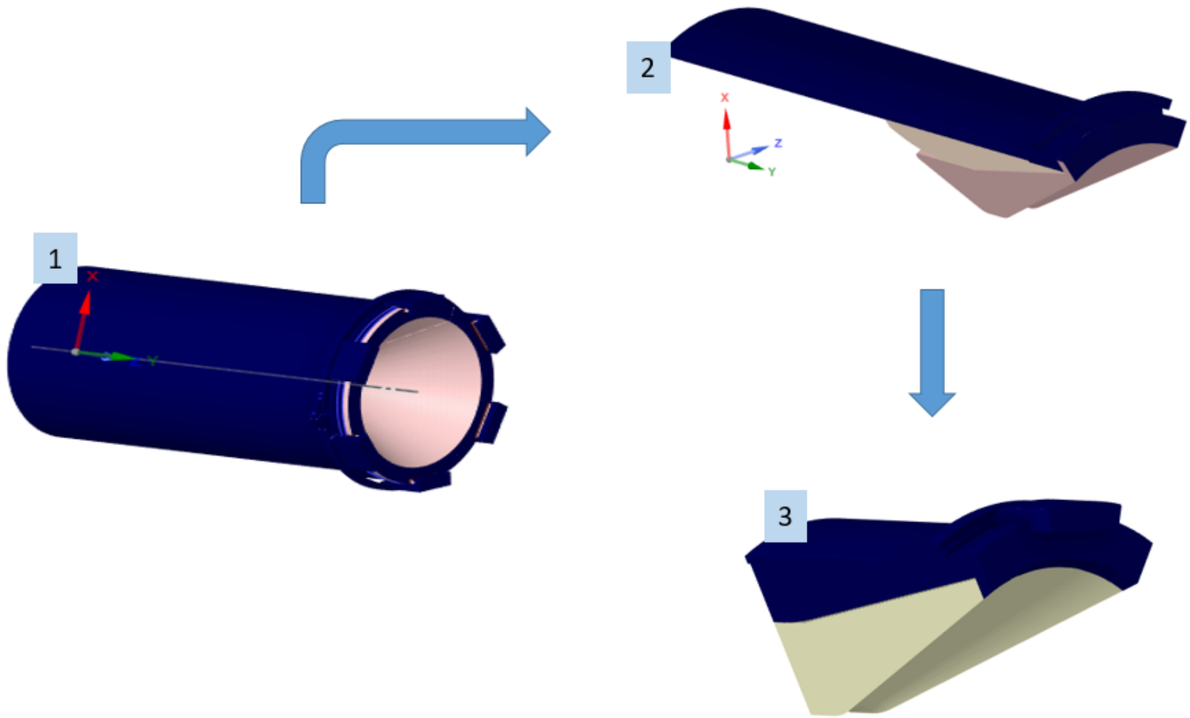

Figure 2. Slice image of the model

The numbers of "nodes" and "elements" obtained in the mesh study (same size and same mesh model) on Models 2 and 3 are given in Figure **3** and Figure **4**. Model 2 has approximately 450,000 elements, while model 3 has approximately 210,000 elements.

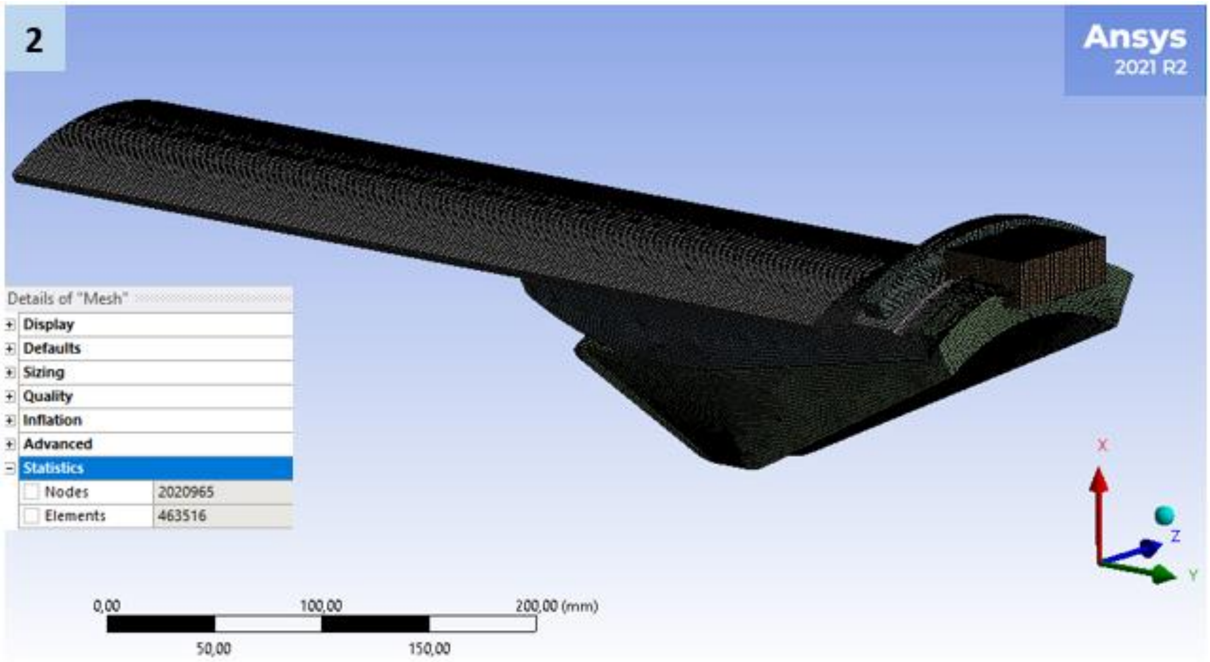

Figure 3. Number of elements and nodes obtained on model number 2

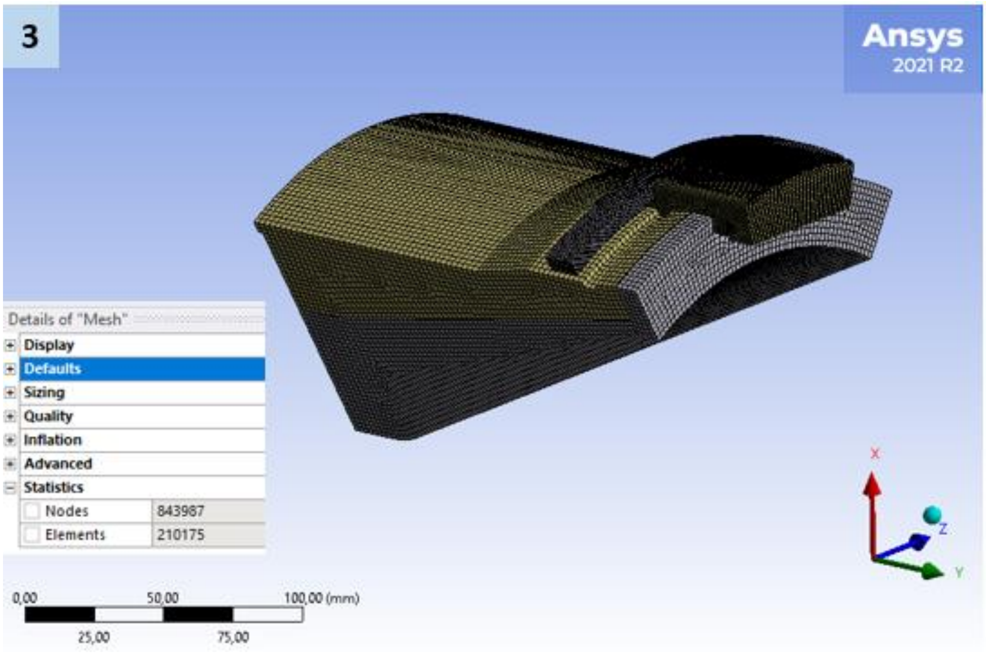

Figure 4. Number of elements and nodes obtained on model number 3

<u>Material</u>

After determining the suitable model for the analysis, suitable material properties and boundary conditions are defined. In this study, separable nozzle material was chosen as Sifet (Silica phenolic composite). The reason for this situation is the flow at high flow rate and temperature to which it will be exposed in the accelerating phase. Sifet material is frequently used as an insulation material in the aviation industry due to its resistance to heat. Other parts of the engine assembly are assigned as 4140 Steel material. The material information of the model is given in Figure **5**. Material properties are given in Table **1** and Table **2**.

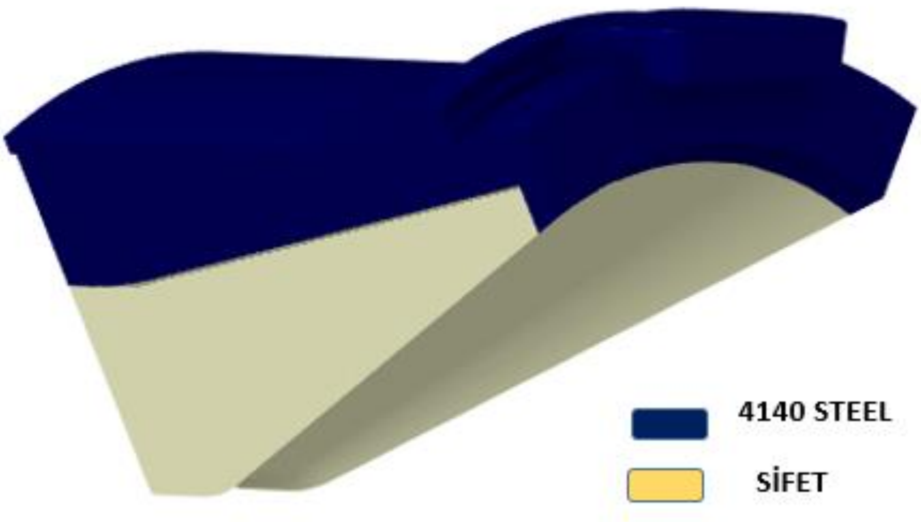

Figure 5. Material information of parts

Table 1. Material properties of 4140 steel

4140 Steel	
Density (kg/m^-3)	7850
Young's Modulus (Gpa)	200
Poisson's Ratio	0,32
Coefficient of Thermal Expansion (C^-1)	1,23^-05
Tensile Yield Strength (Mpa)	1000
Tensile Ultimate Strength (Mpa)	1100

Table 2. Material properties of Sifet

Sifet	
Density (kg/m^-3)	1650
Young's Modulus (GPa)	9,4
Poisson's Ratio	0,15
Coefficient of Thermal Expansion (C^-1)	7,75^-06
Tensile Yield Strength (Mpa)	250
Tensile Ultimate Strength (Mpa)	460

Connections

5 different connection types are defined in the ANSYS program; Bonded, No Separation, Frictionless, Rough and Frictional. Descriptions of these connection types are given below [ANSYS, 2002].

Bonded

If Bonded is used on the contact surfaces, no sliding or separation is allowed between the faces or edges. The region is considered either glued or welded. This type of contact allows a linear solution as it will not change the contact length or area during application of the load. Since the pieces are considered to be adhered, they cannot be moved on the surface both in the normal direction and in the tangential direction. The constraints of the part movement are shown in Figure **6**.

Figure 6. Bonded connection type

No Separation

With this type of contact, sliding/tangential movement is possible, but nodes in contact are connected in the normal direction to the target surface and movement in the normal direction is not possible. During the analysis, the contact surface and the target surface remain connected. The constraints of the part movement are shown in Figure **7**.

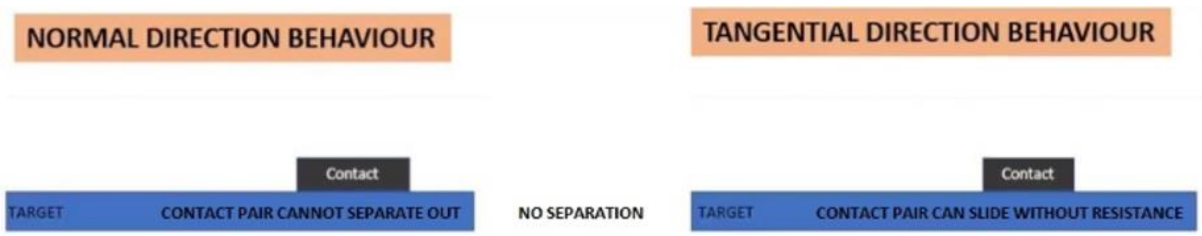

Figure 7. No Separation connection type

Frictionless

The connecting surface can slide tangentially over the target surface and seperate in the normal direction. The coefficient of friction is not defined. Thus, free sliding is allowed. The constraints of the part movement are shown in Figure **8**.

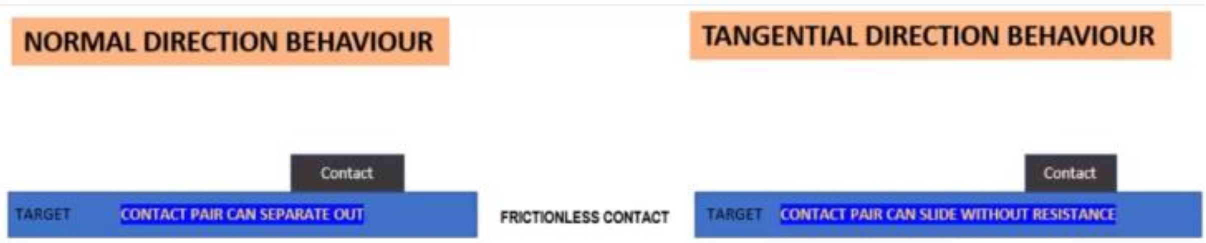

Figure 8. Frictionless connection type

Frictional

The connecting surface can slide tangentially over the target surface and split in the normal direction. Friction coefficients affect tangential motions. If the shear stress due to the frictional force is exceeded, the two geometries will slide relative to each other. The friction coefficient can be any number that is not negative. The constraints of the part movement are shown in Figure **9**.

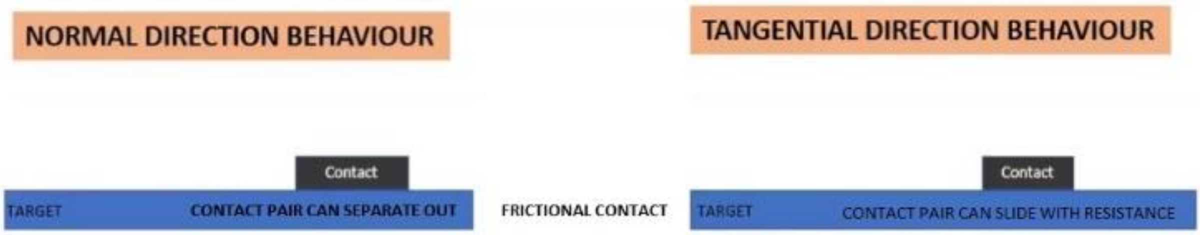

Figure 9**.** Frictional connection type

<u>Rough</u>

The connecting surfaces can be separated from each other in the normal direction, but not in the tangential direction, because the contact surface is adhered in the tangential direction to the target surface. The constraints of the part movement are shown in Figure **10**.

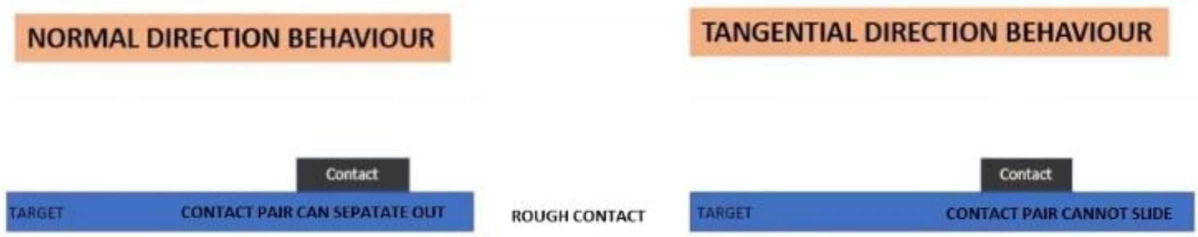

Figure 10. Rough connection type

In this study, the type of connection between all parts of the assembly is defined as Frictional. The Frictional Coefficient value between parts was accepted as 0.2.

Boundry Conditions

If the model of the problem to be analyzed contains symmetrical features, it was discussed in the previous sections since a smaller analysis geometry could be used by specifying the boundaries on which symmetry could be defined on the model. In this way, results can be obtained in a short time by using fewer elements. Since the designed rocket assembly has a symmetrical structure, continuing the analysis by taking the slice structure will give the same result as solving the whole body. In this part, the surfaces given in Figure **11** are selected and defined as frictionless support.

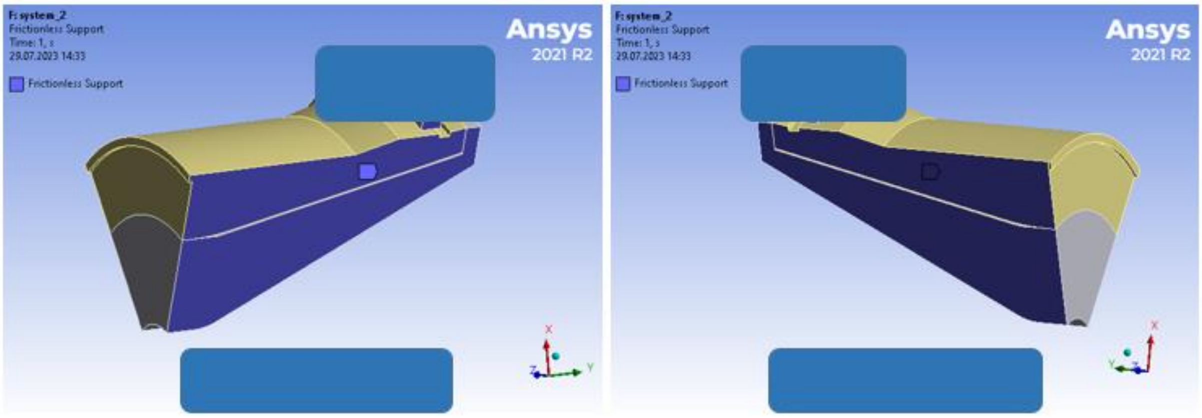

Figure 11. Identified frictionless support surfaces

As the analysis boundary condition, the rear of the engine is defined as the fixed support as given in Figure **12**.

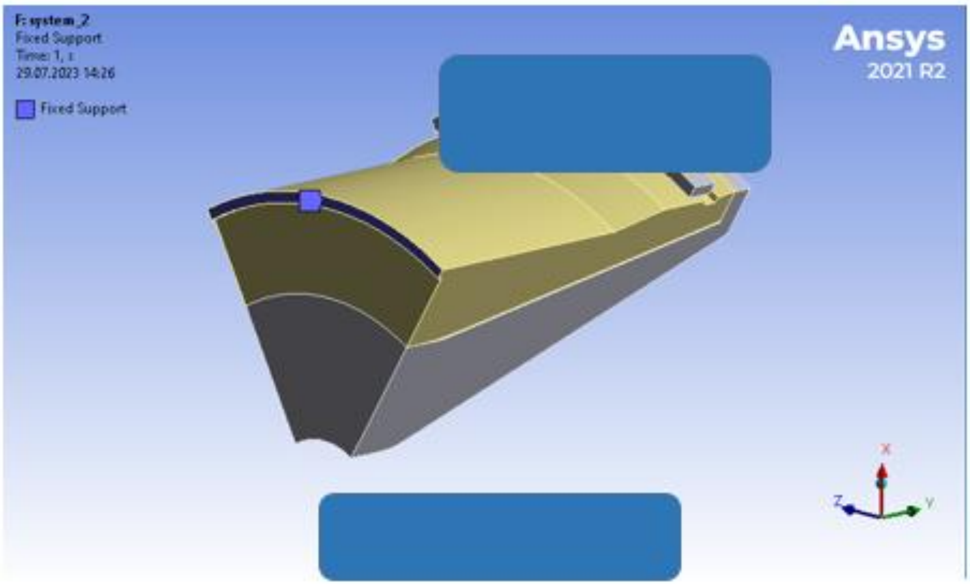

Figure 12. Identified fixed support surfaces

In rocket engines, the compressed gas formed as a result of the combustion of the fuel comes out of the nozzle and produces thrust. The internal pressure value of the engine, obtained as a result of the ballistic combustion analysis, is reflected on the interior volume surfaces as shown in Figure **13**. This pressure value is approximately 12MPa at the nozzle inlet and 1.5MPa at the nozzle outlet.

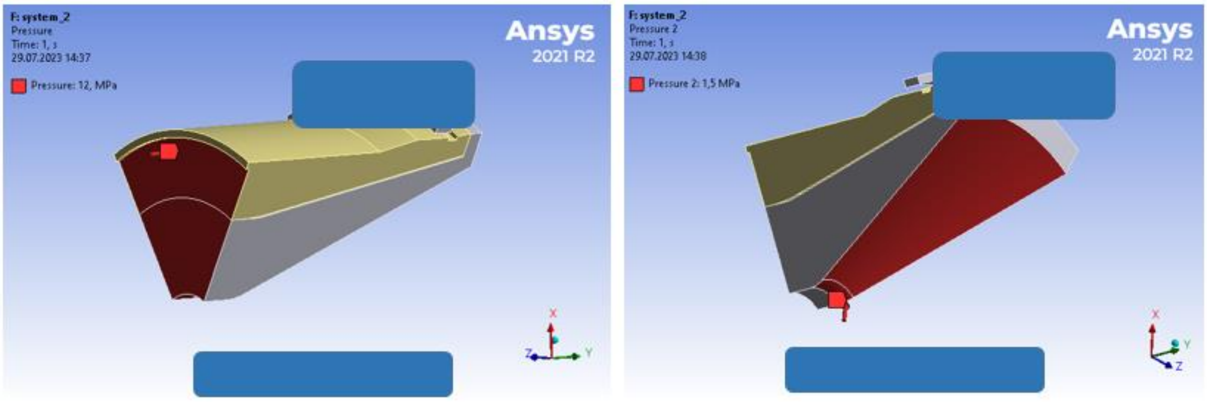

Figure 13. Engine Assembly inner surface pressure distribution

Improvements on holder part designs are performed by using conventional engineering approaches in the first stage. The geometry (holder and clamp parts) designed in rough form is gradually improved according to the analysis results and an acceptable design is obtained before starting the topology optimization. Different design studies of the holder and clamp part can be seen in Figure **14**.

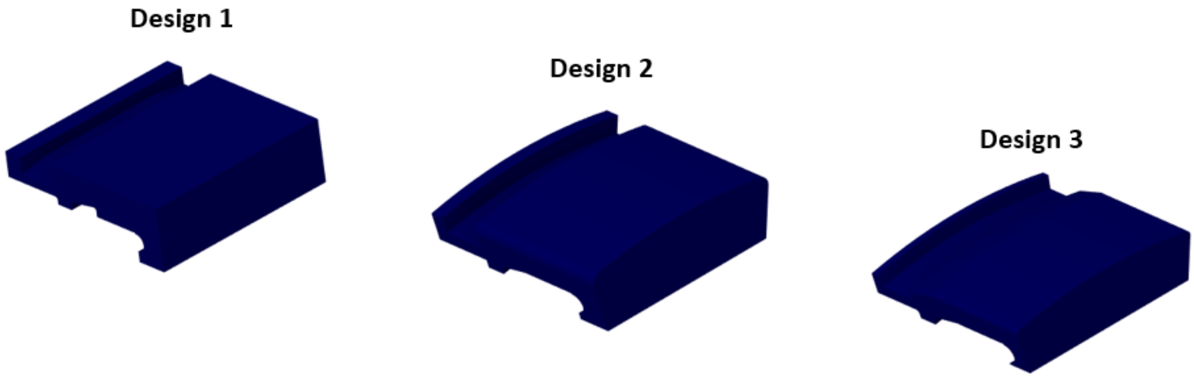

Figure 14. Different design studies of the holder and clamp part

Structural Analysis Results

The results obtained from the mentioned analysis studies are shown in Figure 15 through 21, where the stress distributions in the holder and clamp parts are depicted. Note that the parts are produced from 4140 steel, having a yield strength of 1000 MPa, and tensile strength of 1100 MPa. The parts are produces from Sifet, having a yield strength 250 MPa, and tensile strength of 460 MPa. Firstly, the holder and clamp piece designed in rough dimensions are analyzed. The stress values obtained are smaller than the strength of the parts. In the second and third design studies, the thicknesses of the parts subjected to low stresses and having high strengths are reduced iteratively.
When the analysis results of Design 3 are examined (see Figure 17), it is seen that the stress values in the sharp corner regions exceed 1000 MPa. However, the results are evaluated as regional and it is considered that the piece is high likely to preserve its integrity.

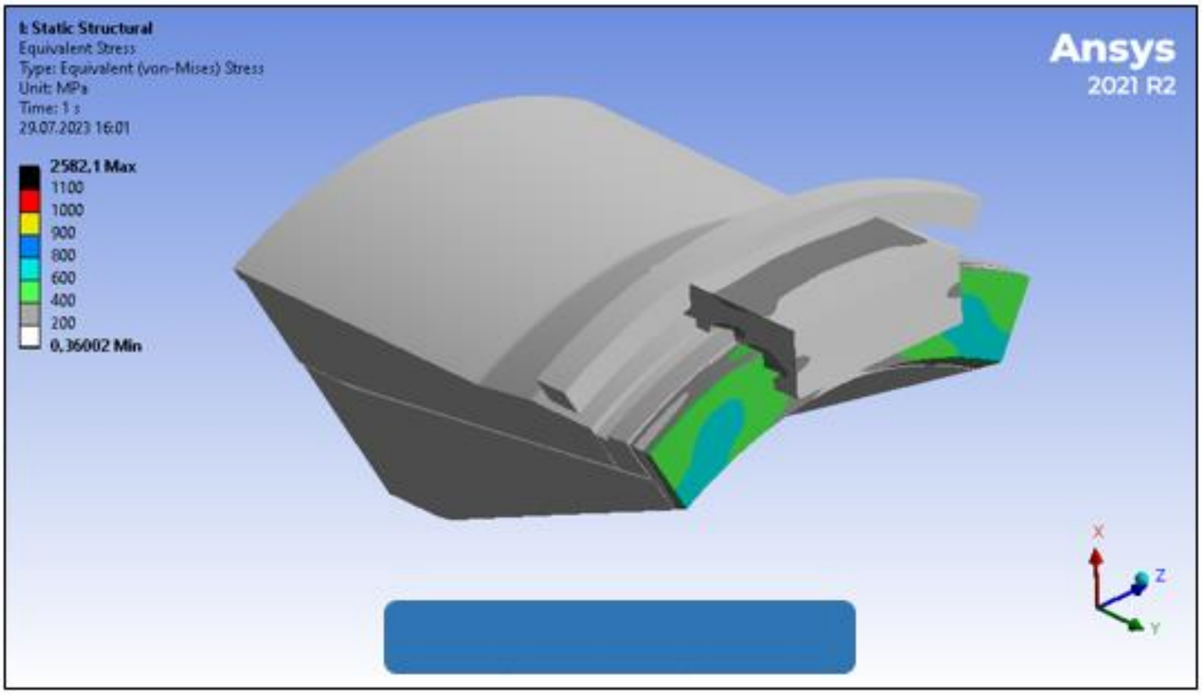

Figure 15. Analysis studies applied to design 1

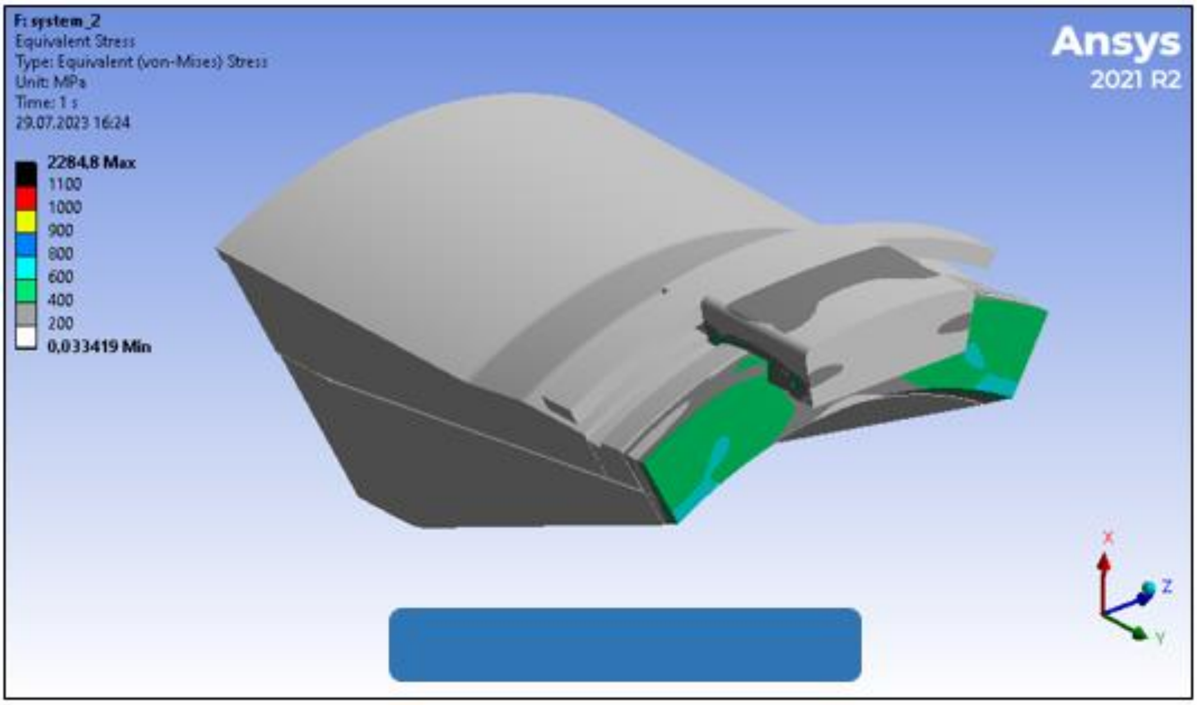

Figure 16. Analysis studies applied to design 2

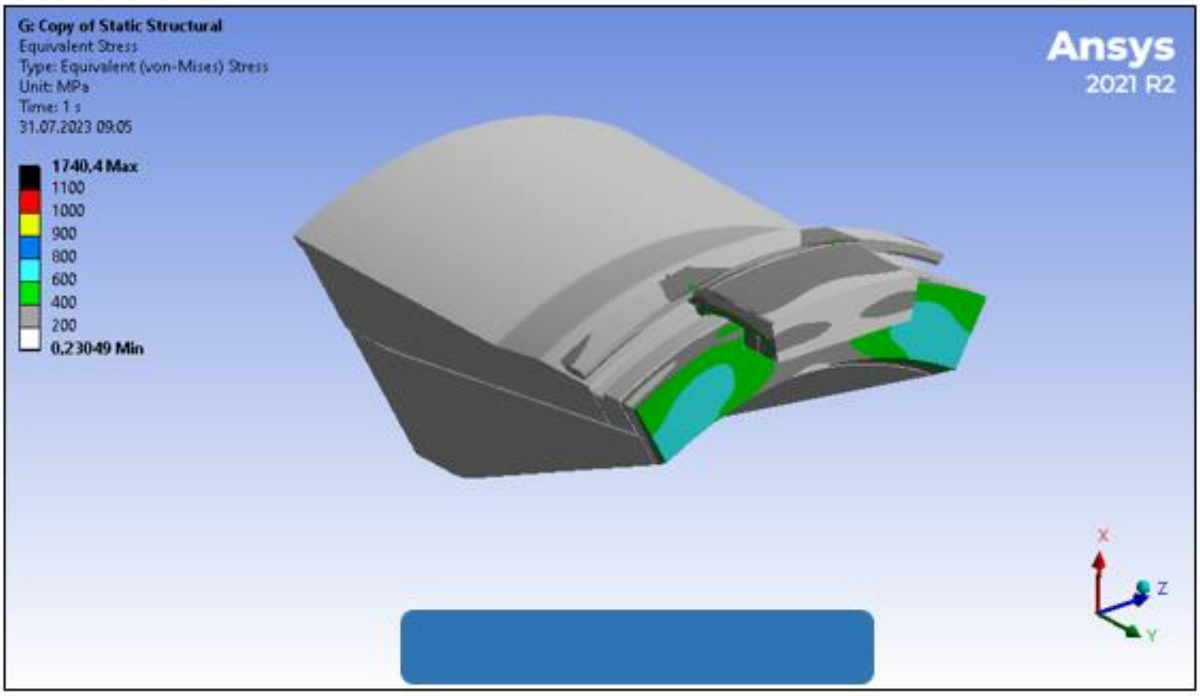

Figure 17. Analysis studies applied to design 3

At the end of the analysis, the stress values obtained for the design no. 3 are close to the material strength. Therefore, the final design has been reached in the holder and clamp parts. After this stage, the production of holder and clamp parts was carried out.

Hidrostatic Tests

The finished parts were then mounted on the engine assembly and pressure tested. In the pressure test, a pressure of 12 MPa was applied by the aqueous pressure system. The pressure test assembly is shown in Figure **18**.

Figure 18. Assembly of Holder and Clamp part

The pressure test was carried out in the aqueous test system. HPL-1200 model power unit produced by “Hidroplus Mühendislik” was used for the pressure test. Technical information of the power unit and the unit image are given in Figure **19**.

Figure 19. Pressure Test Unit

In order to perform the pressure test, the piping system of the pressure unit is connected to the appropriate interfaces on the motor body. In this way, pressurized water pressurizes the internal volume of the engine pipe. For the safety of the tests, the tests were carried out in the safety cabinet. The visuals of the test assembly and the test cabin are given in Figure **20** and Figure **21**.

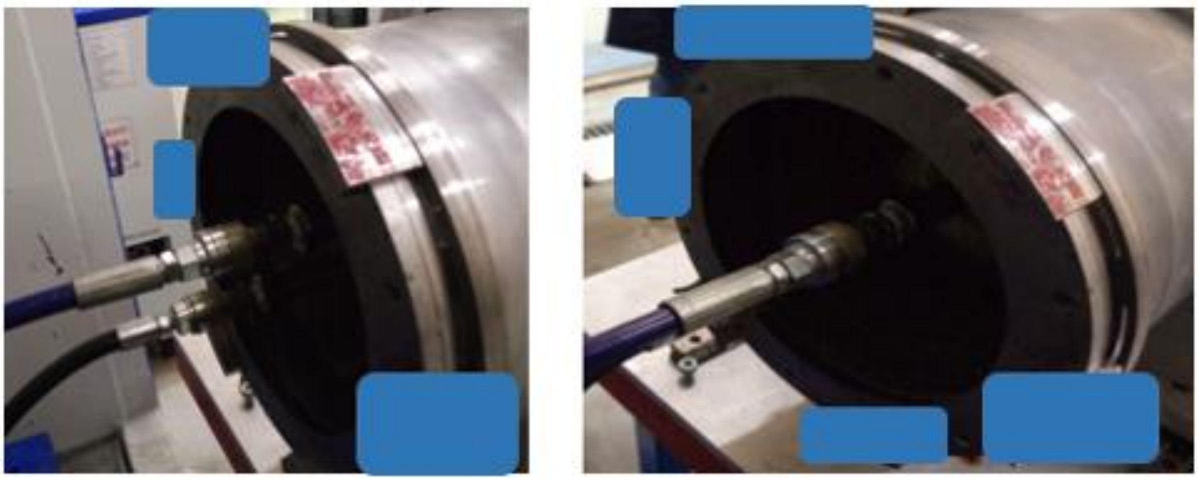

Figure 20. Pressure Test Assembly

Figure 21. Pressure Test Cabinet

The control panel of the hydrostatic pressure system is given in Figure **22**. First, pre-filling was done through the system. After the pre-filling was completed, a two-stage pressure test was performed.

Figure 22. Pressure Test System Control Board

In the first step, the pressure value was entered as 870 PSI (6 MPa). The test set, which was pressurized to 870 PSI, was kept at this pressure value for 20 seconds. Then, the pressure was cut off and it was checked that there was no leakage or deformation on the test assembly. In the second step, the test pressure value was entered as 1740 PSI (12 MPa). The test set, which reached a pressure value of 1740 PSI, was kept at this pressure value for 20 seconds. Then the test was terminated. The pressure-time graph of the test is given in Figure **23**.

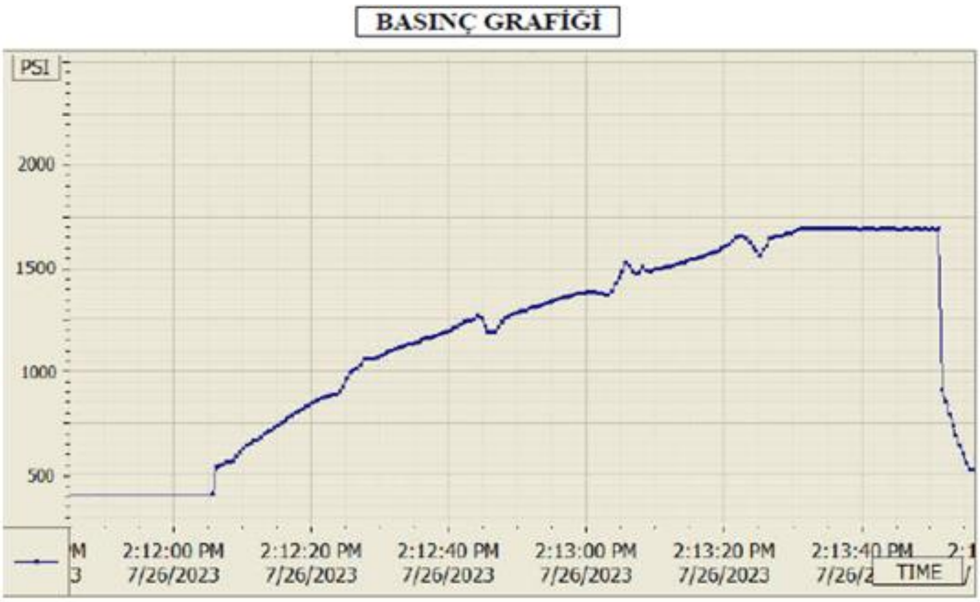

Kademe	Test Süresi	Basınç Değeri	Max. Basınç	Fark Basınç
1	20 sn.	+1740.000 psi	+1814.562 psi	+74.562 psi
2	10 sn.	+580.000 psi	+0.000 psi	+0.000 psi
3	10 sn.	+725.000 psi	+0.000 psi	+0.000 psi
4	10 sn.	+870.000 psi	+0.000 psi	+0.000 psi
5	10 sn.	+1160.000 psi	+0.000 psi	+0.000 psi
6	0 sn.	+0.000 psi	+0.000 psi	+0.000 psi
7	0 sn.	+0.000 psi	+0.000 psi	+0.000 psi
8	0 sn.	+0.000 psi	+0.000 psi	+0.000 psi
9	0 sn.	+0.000 psi	+0.000 psi	+0.000 psi
10	0 sn.	+0.000 psi	+0.000 psi	+0.000 psi

Figure 23. Pressure - Time Graph

Topology Optimization

After the initial design was verified, a topology optimization study was carried out on the relevant parts. Two different solution methods as Density Method and Homogenization Method are used in topology optimization solutions. In this study, the Density Method was used as the optimization method. In this method, it assigns an intensity value between 0 and 1 to each element in the FEA model. The element with a density value of 0 is removed from the part, while the element with a density value of 1 remains in the part.

After determining the boundary conditions for optimization on the model, the type of topology optimization should be determined. There are 3 different topology optimizations in ANSYS 2021 R2 version. These are mass discharge, volume discharge and Global Von-Mises stress discharge. In this study, mass discharge was preferred as the analysis input, since it was aimed to reduce the maximum mass without weakening the part strength.

After the appropriate method is determined, the amount to be discharged must be entered into the program. For this, the rate to be discharged is entered as 70% in the “Percent to Retain” section. This value means 30% mass discharge from the part. The geometry obtained as a result of the analysis is shown in Figure **24**.

Figure 24. Geometry obtained as a result of topology optimization

The mass and volume values of the final piece and the first piece obtained as a result of the analysis are given in Figure **25**.

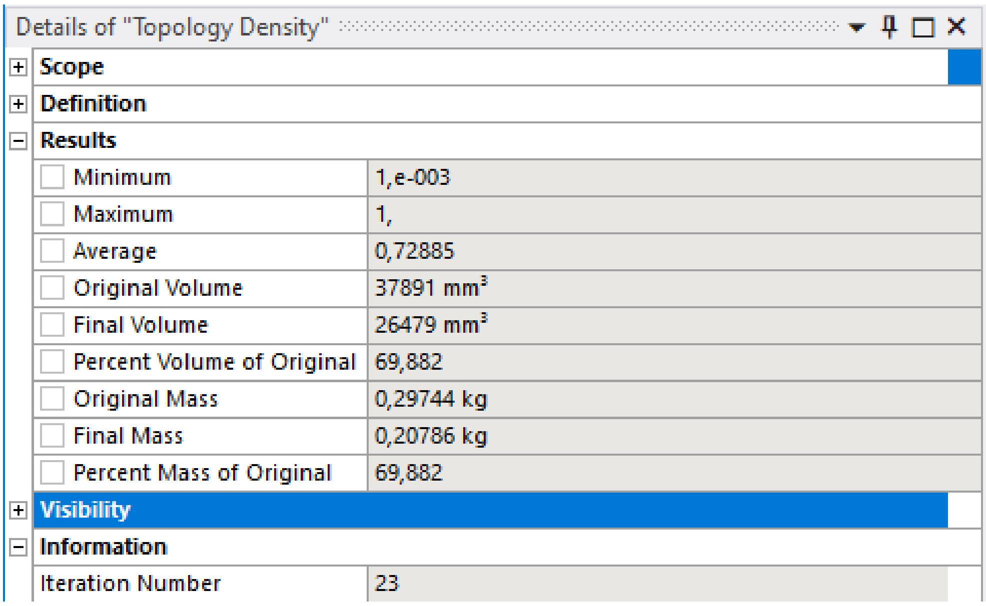

Details of "Topology Density"

Scope	
Definition	
Results	
Minimum	1,e-003
Maximum	1,
Average	0,72885
Original Volume	37891 mm³
Final Volume	26479 mm³
Percent Volume of Original	69,882
Original Mass	0,29744 kg
Final Mass	0,20786 kg
Percent Mass of Original	69,882
Visibility	
Information	
Iteration Number	23

Figure 25. Mass and volumetric comparison of the first and last part

The parts removed from the part as a result of topology optimization are shown in blue in Figure **26**. Here, the parts shown in red are the parts that are not removed from the part.

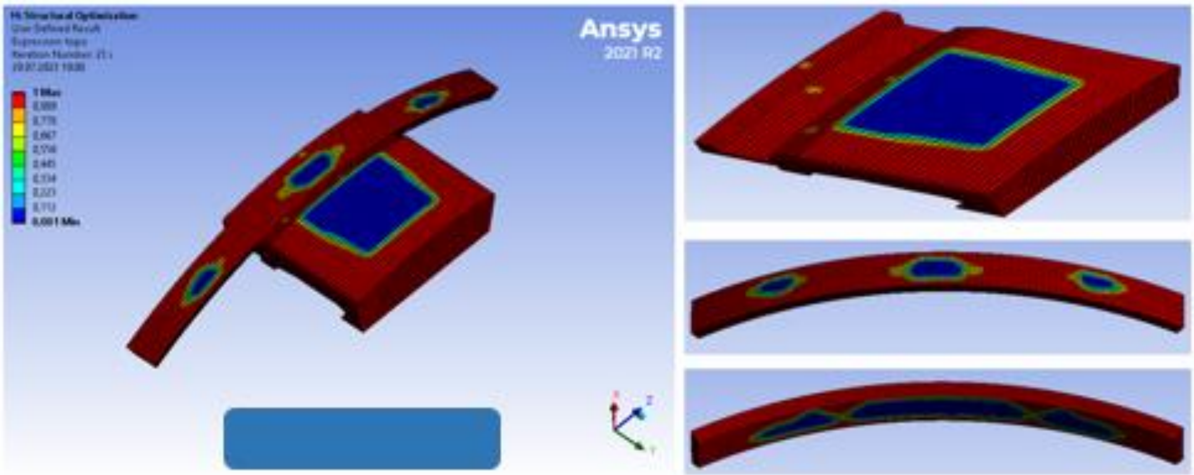

Figure 26. As a result of topology optimization, removed and unremoved regions from the part.

The part obtained after the topology optimization was transferred to SpaceClaim, making the part more suitable for production and remodeled. The visuals of the modeled geometry and the placement of the new model on the complete are given in Figure **27**.

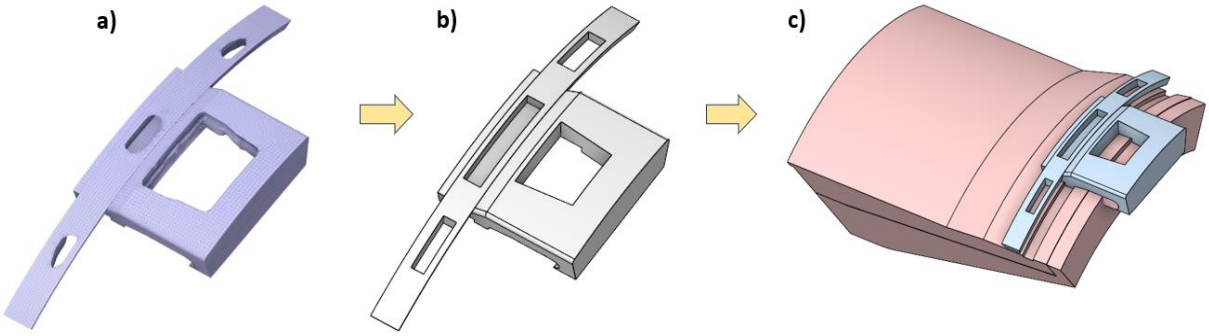

Figure 27. a) The geometry obtained as a result of topology optimization. b) Geometry edited in SpaceClaim. c) Assembly view of the final version of the holder and clamp part

The model designed according to the topology optimization result was analyzed under the same boundary conditions with the main part. As a result of the static analysis, the maximum equivalent (von-Mises) stress value of the part was found to be 1670 MPa. The visual of the analysis result is given in Figure **28**.

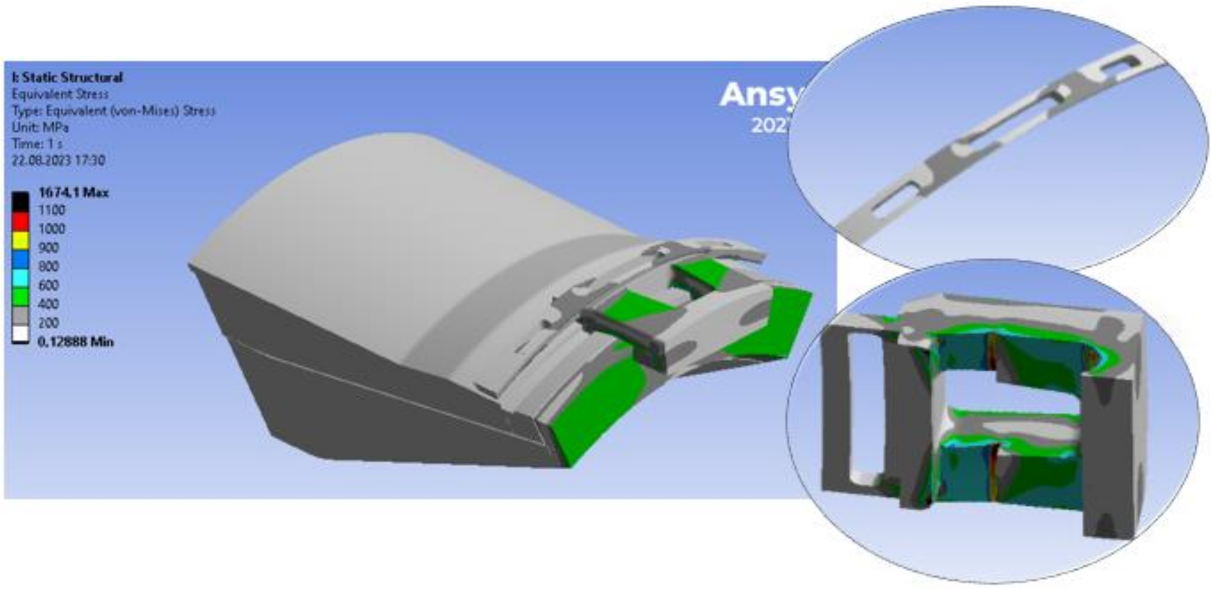

Figure 28. Maximum von-Mises stress value of the design

CONCLUSION

In this study, it is aimed to improve the design of the nozzle separator part used for the two-stage rocket engine. The design work was first carried out in 3 stages using CATIA software. Structural analysis was performed using ANSYS finite element software for the model obtained after the first design. In this design, local stress accumulation was high (2580 MPa), since the area where the gripper part comes in contact with the motor body has a limited surface area. In line with the results obtained, improvements were made on the part with an engineering approach. In the improved design, the contact surface between the holder and the motor body has been increased and it has been re-analyzed. As a result of the analysis, the maximum equivalent (von-Mises) stress value has increased to 2280MPa. In line with the analysis results obtained, some sharp corners were designed in circular form and the 3rd Design was obtained. 3. In the design, the maximum equivalent (von-Mises) stress value on the part is seen as 1740MPa. Although this value seems to exceed the yield strength of 4140 steel normally, the resulting stress value has occurred in local areas at the corner points. To verify the final design (3rd Design) obtained, hydrostatic pressure tests were performed and the part was held under 12MPa pressure for 20 seconds.

The next design improvement studies were carried out using the Topology Optimization tool in the ANSYS program. The necessary boundary conditions were defined in the analysis program and the design was improved. Afterwards, the obtained model was transferred to SpaceClaim and the geometry was edited considering the part manufacturability. The obtained corrected geometry was transferred to the ANSYS structural analysis program and solved under the same boundary conditions. The stress value seen on the piece obtained after the optimization study is around 1290MPa. Although it exceeded the yield strength of the steel at this value, it was interpreted as locality and it was evaluated that the part would show strength. As a result of the optimization study, approximately 30% mass improvement was achieved in the clamp and holder part.

References

Aminjan, K.K (2022) ***"****Thermodynamic Analysis of Ramjet Engines and its Optimal Functional Conditions"* The Splendid Journals, August 2022

ANSYS (2002) Ansys Advanced Analysis Techniques Guide: release 6.1. February 2002

Fry, R.S. (2004) *"A century of Ramjet Propulsion Technology evolution"* Journal of Propulsion and Power, 20(1), pp. 27–58., May 2004

Jiang, T., & Chirehdast, M. (1996) A systems approach to structural topology optimization: Designing optimal connections. *Volume 3: 22nd Design Automation Conference*. August 1996

Rozvany, G. I. (2008) A critical review of established methods of structural topology optimization. *Structural and Multidisciplinary Optimization*, *37*(3), 217–237. February 2008

WEBSTER, F. (1978) *"Liquid fueled Integral Rocket/Ramjet Technology Review,"* 14th Joint Propulsion Conference, August 1978